Magnetocardiographic Assessment of Healed Myocardial Infarction

Helena Hänninen, M.D.,*† Miia Holmström, M.D.,‡ Paula Vesterinen, M.D.,*† Milla Karvonen, B.Sc.,†§ Heikki Väänänen, M.Sc.,§ Lasse Oikarinen, M.D.,*† Markku Mäkijärvi, M.D.,* Jukka Nenonen, Ph.D.,†§ Kirsi Lauerma, M.D.,‡ Toivo Katila, Ph.D.,§ and Lauri Toivonen, M.D.*

From the Division of Cardiology, †BioMag Laboratory, and ‡Department of Radiology, Helsinki University Central Hospital; Helsinki, Finland; and §Laboratory of Biomedical Engineering, Helsinki University of Technology, Espoo, Finland

Background: We evaluated the capability of multichannel magnetocardiography (MCG) to detect healed myocardial infarction (MI).

Methods: Multichannel MCG over frontal chest was recorded at rest in 21 patients with healed MI, detected by cine- and contrast-enhanced magnetic resonance imaging, and in 26 healthy controls. Of the 21 MI patients, 11 had non-Q wave and 10 Q wave MIs. QRS, ST-segment, T wave and ST-T wave integrals, ST-segment and T wave amplitudes, and QRS and ST-T wave magnetic field map orientations were measured.

Results: The MCG repolarization indexes, such as ST segment and ST-T wave integrals, separated the MI group from the controls (ST-T wave integral -1.4 ± 5.3 vs 1.5 ± 4.7 pTs, $P = 0.034$). The abnormalities were more distinct in the Q wave-MI than in the non-Q wave MI subgroup. In the latter, however, a trend similar to the Q wave MI group was found. The relation of QRS area to ST segment and T wave integral improved the detection of healed MIs compared to the ST-T wave indexes alone (QRS-ST-T discordance 14 ± 10 vs 5.0 ± 7.1 pTs, $P = 0.003$). When comparing the MI group to the controls, the orientation of the magnetic field maps differed in the ST-T wave maps ($163 \pm 119^\circ$ vs $58 \pm 17^\circ$, $P < 0.001$) but not in the QRS maps ($111 \pm 95^\circ$ vs $106 \pm 93^\circ$, $P = 0.646$).

Conclusions: The MCG repolarization variables can detect healed MI. These ST-T wave abnormalities are more pronounced in patients with Q wave MI than in patients with non-Q wave MIs. Relating the signals of depolarization and repolarization phases improves the detection of healed MI. Repolarization abnormalities are common in healed MI and thus should not always be interpreted as present ongoing ischemia.

A.N.E. 2006;11(3):211–221

coronary artery disease; magnetic resonance imaging; magnetocardiography; myocardial infarction

Acute coronary syndrome is the second most common cause of hospital admission in industrialized countries. The most effective approach for the high-risk coronary patients is invasive treatment strategy early after hospital admission.[1] Detection of ongoing ischemia in patients with a history of myocardial infarction (MI) remains a diagnostic challenge, due to preexisting abnormalities in the electrocardiogram (ECG). Identifying the extent of ischemic but retrievable myocardium as opposed to necrotic scar areas is of primary importance in assessing the achievable benefits of revascularization.

Multichannel magnetocardiography (MCG) is a novel, noninvasive mapping technique to register the extracorporeal magnetic field of the heart, generated by the cellular ionic currents. Interestingly, MCG is less affected by attenuation due to the intervening thoracic tissue than is the electric field.[2] Recent development in the MCG instrumentation has allowed MCG recordings to be made in

Address for reprints: Helena Hänninen, M.D., Helsinki University Central Hospital, Division of Cardiology, Cardiovascular Laboratory, P.O. Box 340, Fin 00029 Huch, Finland. Fax: +358 9 4717 4574, E-mail: helena.hanninen@welho.com

This work was supported by grants from the Finnish Cardiac Research Foundation and Aarne Koskelo Foundation.

Table 1. Clinical Characteristics of the Study Groups

	Number	Age (Years)	Male/Female	LVEF (%)	Heart Rate (Beats/Min)	Body Mass Index (kg/m^2)	Age of MI (Years)
All MI	21	62 ± 9	18/3	50 ± 15	62 ± 10	26.3 ± 4.1	7.1 ± 8.6
NQMI	11	62 ± 12	9/2	56 ± 12	59 ± 6	26.6 ± 4.4	7.7 ± 9.3
QMI	10	62 ± 6	9/1	43 ± 15	64 ± 12	25.9 ± 3.9	6.3 ± 8.4
Controls	26	51 ± 10	20/6	66 ± 7	68 ± 10	24.6 ± 3.8	–

Number of study subjects or mean ± standard deviation. LVEF = left ventricular ejection fraction; MI = myocardial infarction; NQMI = non-Q wave myocardial infarction; QMI = Q wave myocardial infarction.

the hospital environment.[3,4] Lately, MCG research has focused on detection of transient ischemia.[4–9] We evaluated the electrophysiological abnormalities produced by healed MI in MCG mapping and applied cine- and contrast-enhanced magnetic resonance imaging (MRI) as a reference method.

METHODS

Study Subjects

The study population (n = 47) consisted of two groups. The MI group (n = 21) included patients with a history of one or more healed MIs. The MI was defined as a history of chest pain suggestive of MI together with increased creatine kinase MB fraction (>10 IU/L and >5% of the total creatine kinase) (MI group) (Table 1). In addition, the inclusion also required the presence of MI scar region in cine- and contrast-enhanced MRI at the time of the study. All patients had at least one significant (≥70%) stenosis in coronary arteriography. None of the patients had unstable coronary artery disease, and they all were symptom-free at the time of the MCG recording. In all MI patients, the timeframe between MKG and MRI investigations was less than 2 weeks.

The control subjects (n = 26; controls) were healthy middle-aged volunteers who had no coronary risk factors and no history or signs of cardiovascular disease (Table 1). They underwent symptom-limited bicycle exercise test without angina or ST-segment changes and had a normal echocardiogram.

All study subjects were in sinus rhythm and none showed a bundle branch or a fascicular block in the ECG. The study protocol was approved by the ethical committee of the Helsinki University Central Hospital, and informed consent was obtained from all the participants.

MRI and Image Analysis

All patients eligible to the MI group underwent cine- and contrast-enhanced MRI to assess the localization and extent of the infarcted myocardium. Patients were positioned supine on the table of a 1.5-T imager (Magnetom Vision; Siemens, Erlangen, Germany) and imaging was performed with a body array coil as a receiver. Transverse, oblique sagittal, and double-oblique left ventricular (LV) long-axis scout images were obtained to determine the final short-axis imaging plane. A LV short-axis orientation was selected for MRI to minimize partial volume effects. Five short-axis sections of 10 mm thickness 15 mm apart were registered with a electrocardiographically gated cine-MRI, which produces a series of LV wall images within cardiac cycle every 40 ms. The perfusion of the LV wall of the same sections was imaged during contrast agent injection (0.05 mmol/kg gadopentetate dimeglumine, Magnevist; Schering, Helsinki, Finland) and the late enhancement of the myocardium was observed for 20 minutes with an inversion recovery turboFLASH sequence.[10] The larger extracellular volume in the infarcted myocardium appears as increased signal intensity during the late enhancement period.

When the diastolic wall thickness was less than 5.5 mm, there was less than 2 mm systolic thickening, or there was significant late enhancement of more than two standard deviations (SD) of normal myocardium, the myocardial segment was classified to be infarcted.[10]

MI Classification

ECG

In order to relate the patient population to standard epidemiological means of MI diagnosis, the patients were divided into two subgroups according

to Minnesota code criteria:[11] Q wave myocardial infarction (QMI) group comprising 11 patients and non-Q wave myocardial infarction (NQMI) group comprising 10 patients (Table 1). Codes 1-1 and 1-2 in the 12-lead ECG defined QMI. In coronary arteriography significant stenosis were distributed in all three major artery branches.

MRI

According to the American Heart Associations (AHA) recommendation of LV segmentation, the myocardium was divided into 16 segments, and these segments were combined to form four anatomical MI regions.[12–14] By assigning one patient into more than one group, altogether 9 patients had MI in anterior, 10 patients in apical, 4 patients in lateral, and 13 patients in inferoposterior region.

Magnetocardiography

Multichannel MCG, covering a circular area of a diameter of 30 cm over the precordium, was recorded for 5 minutes.[15] The signals were selectively averaged and processed to obtain MCG data of one cardiac cycle in 33 recording locations[16] (Fig. 1).

By use of an algorithm based on a method originally presented by Simson for QRS onset and offset identification, and a previously validated algorithm for determination of T wave fiducial points, the QRS onset and offset, and T wave offset in each location were determined.[17,18] Medians of all signals were calculated for QRS onset, QRS offset, and T wave offset times and applied to define the time instants for measuring the amplitudes and the start and the end of the integrals in all channels. From the signal-averaged MCG data, the following indexes were calculated.

Integrals

QRS Integral

In all channels, the QRS integral was calculated as the time integral from the QRS onset to QRS offset (Fig. 2).

QRS Sextiles

In all channels, the QRS integral was divided into six temporally equal time integral segments, referred as QRS sextiles.

QRS Area

In all channels, the QRS area was calculated as the sum of the absolute values of Q, R, and S wave areas (Fig. 2).

ST-Segment Integral

In each channel, the ST-segment integral was obtained as the time integral from QRS offset to the midpoint between QRS offset and T wave offset.

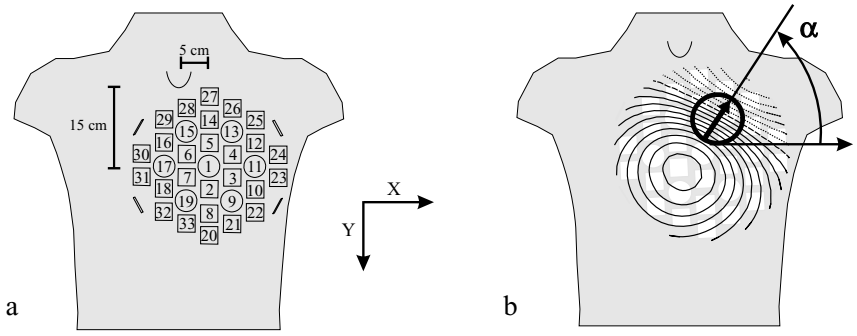

Figure 1. (A) Sensor arrangement and positioning of the cardiomagnetometer with 33 recording locations in relation to the thorax. The device was placed anteriorly with the center of the device 15 cm caudally from the jugular notch and 5 cm left of the midsternal line. (B) In the magnetic field map, the location and orientation of the steepest spatial change in the signal, the peak gradient, is indicated by an arrow. Solid lines indicate positive values and magnetic flux toward the chest and dotted lines indicate negative values and flux out of the chest. Orientation of the magnetic field was measured as the angle between direction of the peak gradient and horizontal x-axis.

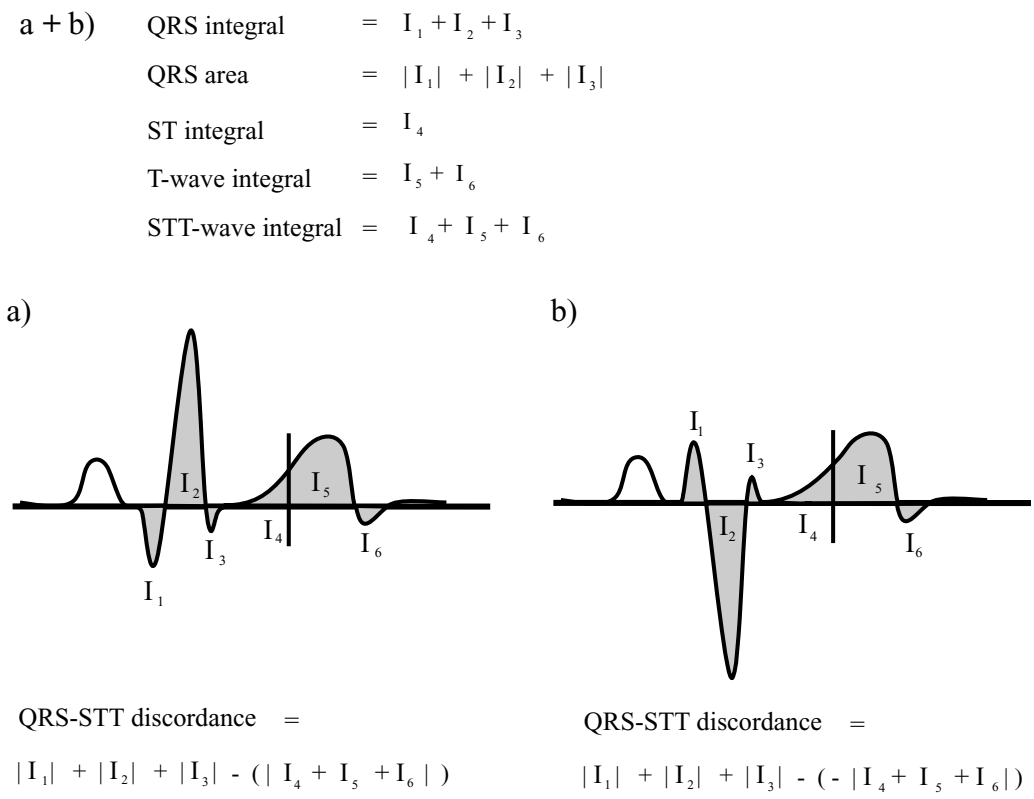

Figure 2. (a + b) Illustration of the calculation of QRS, ST-segment, T wave, and ST-T wave integrals, and QRS-ST-T discordance in each MCG channel. QRS integral was calculated as the time integral from the QRS onset to QRS offset. QRS area was calculated as the sum of absolute values of Q, R, and S wave areas. The ST-segment, T wave, and ST-T wave integrals were obtained as the corresponding time integrals. (a) If the main QRS deflection and the ST-T wave were of same polarity, the ST-T wave integral was subtracted from the QRS area when calculating the QRS-ST-T discordance. The QRS-ST discordance and QRS-T discordance were calculated in an analogous manner. (b) If the main QRS deflection and the ST-T wave were of opposite polarity, the latter was multiplied by −1 when calculating the QRS-ST-T discordance. The QRS-ST discordance and QRS-T discordance were calculated in an analogous manner.

The absolute value of the ST-segment integral was used to assess the QRS-ST discordance (Fig. 2).

T Wave Integral

In each channel, the T wave integral was obtained as the time integral from the midpoint between QRS offset and T wave offset to the T wave offset. The absolute value of the T wave integral was used to assess the QRS-T discordance (Fig. 2).

ST-T Wave Integral

In each channel, the ST-T wave integral was obtained as the time integral from QRS offset to the T wave offset. The absolute value of the ST-T wave integral was used to assess the QRS-ST-T discordance (Fig. 2).

QRS-ST-T Discordance

To combine data of both ventricular depolarization and repolarization, the absolute value of the ST-segment integral (QRS-ST discordance), T wave integral (QRS-T discordance), and ST-T wave integral (QRS-ST-T discordance) was subtracted from the QRS area[19] (Fig. 2A). In channels where QRS integrals and ST, T wave and ST-T wave integrals were of opposite polarity, the latter were considered negative as used previously[18] (Fig. 2B). The rationale of calculating the QRS area and the ST-, T-, and ST-T-integrals differently was based on a

previous study showing that the ECG response to cardiac pathology is flattening of the T wave or polarity reversal of the T wave in relation to the main QRS deflection.[20]

Amplitudes

ST-Segment Amplitude

In each channel, ST-segment amplitude was measured 60 ms after the J point.

T Wave Amplitude

In each channel, T wave amplitude was the amplitude with maximum absolute value from the QRS offset to the T wave offset.

Optimal Recording Locations

To identify the recording locations with the best discriminative power for MI detection, we used departure maps.[21,22] In each channel and for each index, departure map values were calculated by subtracting mean value of the control group from the mean value of the MI group. The obtained difference was then divided by the SD of the control group. The larger the absolute departure map value, the better is the performance of that channel in separating the MI group from the controls. The departure map, thus, allowed the identification of the best recording locations to differentiate between the present study groups.

Magnetic Field Map Orientation

Mean magnetic field maps (MFMs) of the QRS complex and the ST-T wave were formed by calculating the mean of the MCG signal over the mapped area. The MFMs illustrate the spatial distribution of the MCG signal over the mapped area as isofield contours (Fig. 1). Orientations of the MFMs were determined by use of the surface gradient method, described in detail earlier (Fig. 1).[7,19] First, the location of the steepest spatial change of the signal in the MFM was found. Then, the MFM orientation was defined as the direction of the steepest signal amplitude change at that location.

QRS Angle and ST-T Angle

The orientations were determined, in degrees, for the QRS complex (QRS angle) and for the ST-T wave (ST-T angle).

QRS-ST-T Angle Difference

The QRS-ST-T angle difference, in degrees, was calculated as the difference of the orientations of the MFMs of the QRS complex and the ST-T wave.

Electrocardiogram

In a manner analogous to MCG, the sum of QRS area, ST-segment amplitude (60 ms after the J-point), ST-T wave integral and T wave amplitude were calculated over the 12-lead ECG leads.

Statistical Analysis

Statistical data analysis was performed with SPSS version 11.5 software (SPSS, Inc., Chicago, IL, USA). All continuous data are presented as mean $\pm$ SD. The significance of difference between the groups was determined with the Mann-Whitney U test. A 2-tailed P-value ≤ 0.05 was considered statistically significant. Receiver operating characteristic (ROC) curves were created to assess the performance of the parameters in the optimal channels. The results are given as the area under ROC curve (AUC%).

RESULTS

Sums of MCG Parameters Over the Mapping Region

Depolarization Abnormalities in Healed MI

QRS Area: The QRS area was larger in the MI group than in the controls (MI group 15 ± 5.7 pTs vs controls 11 ± 3.7 pTs; $P < 0.042$). The QRS area also separated the QMI subgroup but not the NQMI subgroup from the controls (QMI subgroup 16 ± 6.7 pTs; $P < 0.044$ compared to the controls) (Table 2).

QRS Integral: The QRS integral failed to separate the MI groups from the controls (Table 2). The individual QRS sextiles were not more informative than the whole QRS integral.

Repolarization Abnormalities in Healed MI

ST-Segment Integral: The ST-segment integral did not separate the MI group or the NQMI subgroup from the controls (Table 2). In the QMI subgroup the ST-segment integral was more negative than in the controls (QMI subgroup -1.5 ± 1.8 pTs, controls -0.3 ± 1.2 pTs; $P = 0.037$). The MI group

Table 2. Magnetocardiographic Indexes in Detection of Healed MI

	All MI	P Value	NQMI	P Value	QMI	P Value	Controls
QRS area (pTs)	15.0 ± 5.7	0.042	13.5 ± 4.6	n.s.	16.0 ± 6.7	0.044	11.0 ± 3.7
QRS integral (pTs)	4.5 ± 4.8	n.s.	3.9 ± 0.5	n.s.	5.2 ± 6.6	n.s.	4.3 ± 2.8
ST integral (pTs)	−1.0 ± 1.8	n.s.	−0.5 ± 1.7	n.s.	−1.5 ± 1.8	0.037	−0.3 ± 1.2
T integral (pTs)	−0.4 ± 4.0	n.s.	0.4 ± 4.4	n.s.	−1.4 ± 3.5	n.s.	1.7 ± 3.6
ST-T integral (pTs)	−1.4 ± 5.3	n.s.	−0.09 ± 6.0	n.s.	−2.8 ± 4.4	0.034	1.5 ± 4.7
QRS-ST discordance (pTs)	15.5 ± 6.6	n.s.	14.0 ± 5.7	n.s.	17.0 ± 7.4	0.009	11.0 ± 3.9
QRS-T discordance (pTs)	13.1 ± 8.7	0.004	11.0 ± 9.2	n.s.	15.0 ± 8.0	0.001	5.9 ± 6.2
QRS-ST-T discordance (pTs)	13.9 ± 10.0	0.003	11.5 ± 11.0	n.s.	16.5 ± 9.3	0.001	5.0 ± 7.1
QRS angle (degrees)	111 ± 95	n.s.	134 ± 115	n.s.	87 ± 64	n.s.	106 ± 93
ST-T angle (degrees)	163 ± 119	0.006	110 ± 107	n.s.	220 ± 110	<0.001	58 ± 17
QRS-ST-T angle (degrees)	72 ± 62	n.s.	52 ± 61	n.s.	94 ± 59	0.011	38 ± 46

The values are sums of MI parameters of all channels over the mapped region. Statistical comparisons are made between the MI, QMI, and NQMI patient groups and the control group.
P-values comparing the patient group to the control group; Mann-Whitney U test. Mean ± standard deviation. MI = myocardial infarction; NQMI = non-Q wave myocardial infarction; QMI = Q wave myocardial infarction.

and the NQMI subgroup, however, showed a trend similar to the QMI subgroup but the difference was not significant.

T Wave Integral: The T wave integral did not separate any of the MI groups from the controls (Table 2).

ST-T Wave Integral: The ST-T wave integral did not separate the MI group or the NQMI group from the controls (Table 2). The ST-T wave integral was more negative in the QMI subgroup than in the controls (QMI subgroup −2.8 ± 4.4 pTs, controls 1.5 ± 4.7 pTs; P = 0.034). A trend similar to QMI group was found in the MI group and in the NQMI subgroup.

Depolarization and Repolarization Discordances

QRS-ST Discordance: The QRS-ST discordance was larger in the MI group and in the QMI subgroup than in the controls (MI group 16 ± 6.6 pTs, QMI subgroup 17 ± 7.4 pTs, controls 11 ± 3.9 pTs; P = 0.020, AUC 70% and P = 0.009, AUC 74%, respectively) (Table 2). The NQMI subgroup showed a similar trend to the MI group and QMI subgroup but the difference was not significant.

QRS-T Discordance: The QRS-T discordance was larger in the MI group and in the QMI subgroup than in the controls (MI group 13 ± 8.7 pTs, QMI subgroup 15 ± 8 pTs, controls 5.9 ± 6.2 pTs; P = 0.004, AUC 75% and P = 0.001, AUC 80%, respectively) (Table 2). The NQMI subgroup showed a similar trend to the MI group and QMI subgroup but the difference was not significant.

QRS-ST-T Discordance: The QRS-ST-T discordance was larger in the MI group and in the QMI subgroup than in the controls (MI group 14 ± 10 pTs, QMI subgroup 17 ± 9.3 pTs, controls 5 ± 1.7 pTs; P = 0.003, AUC 76% and P = 0.001, AUC 80%, respectively). The NQMI subgroup showed a similar trend to the MI group and QMI subgroup but the difference was not significant.

Optimal Recording Locations

QRS Integral

The MI groups had larger positive integral values over the inferior part of the mapping region and smaller negative integral values over the superior part of the mapping area than the controls (Figs. 3 and 4). The QRS integral in optimal sites separated the MI group and the QMI subgroup but not the NQMI subgroup from the controls (AUC 71% for the MI group, 77% for the QMI subgroup) (Table 3).

ST-Segment Amplitude

The MI groups had smaller negative values over the inferior part of the mapping region, and larger positive values over the superior part of the

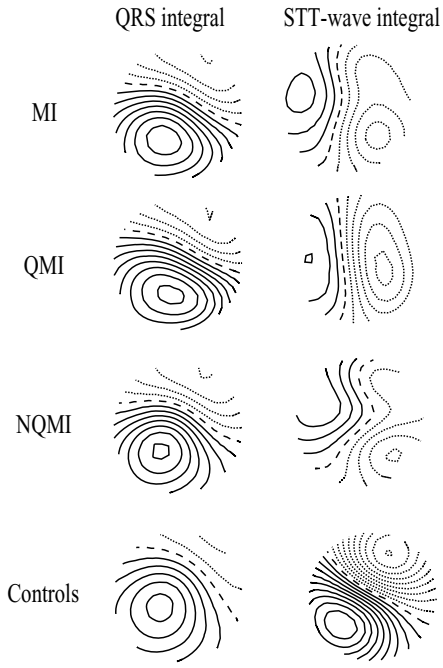

Figure 3. The group mean QRS integral and ST-T wave integral MFMs. From top to bottom: the whole myocardial infarction patient group (MI), the Q wave myocardial infarction subgroup (QMI), the non-Q wave myocardial infarction subgroup (NQMI), and the healthy controls (controls). The QRS integral maps of all patient groups resemble the map of the controls. On the contrary to QRS maps, the ST-T wave integral maps show much more variation in between all the MI groups and the controls. The step between two isocontour lines is 100 pT. Positive values are denoted by solid lines, negative values by dotted lines, and zero field line by dashed line.

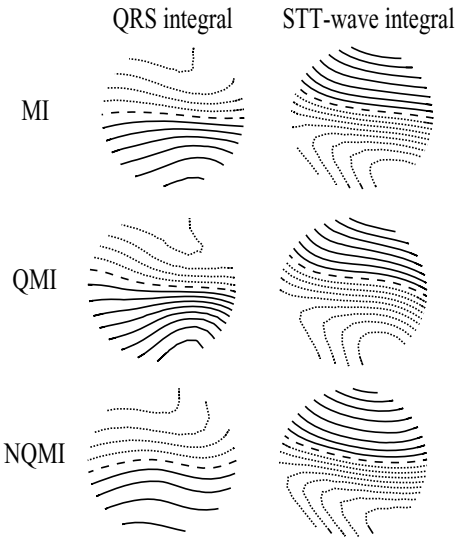

Figure 4. QRS integral and ST-T wave integral departure maps. From top to bottom: the whole myocardial infarction patient group (MI), the Q wave myocardial infarction subgroup (QMI), and the non-Q wave myocardial infarction subgroup (NQMI). In the QRS integral departure maps the MI groups had larger positive values over the inferior part and smaller negative values over the superior part of the mapping region than the controls. In contrast, in the ST-T wave integral departure maps the MI groups had larger smaller negative values over the inferior part and larger positive values over the superior part of the mapping region than the controls. The step between two isocontour lines is 0.25. Positive values are denoted by solid lines, negative values by dotted lines, and zero line by dashed line.

mapping area than the controls. The ST-segment amplitude in the optimal sites separated all MI groups from the controls (AUC 85% for the MI group, 85% for the NQMI subgroup, and 90% for the QMI subgroup) (Table 3).

T Wave Amplitude

The MI groups had smaller negative values over the inferior part of the mapping region, and larger positive values over the superior part of the mapping area than the controls. The T wave amplitude in the optimal sites separated all MI groups from the controls (AUC 91% for the MI group, 91% for the NQMI subgroup, and 92% for the QMI subgroup) (Table 3).

ST-T Wave Integral

The MI groups had smaller negative values over the inferior part of the mapping region, and larger positive values over the superior part of the mapping area than the controls (Figs. 3 and 4). The ST-T wave integral in optimal sites separated all MI groups from the controls (AUC 91% for the MI group, 90% for the NQMI subgroup, and 92% for the QMI subgroup) (Table 3).

Magnetic Field Map Orientation in MI

The QRS angle failed to separate any of the MI groups from the controls (Table 2). The ST-T angle was larger in the MI group and in the QMI subgroup than in the controls (MI group 163 ± 119°, QMI subgroup 220 ± 110°, and controls 58 ± 17°; $P = 0.006$ and $P < 0.001$, respectively). The QRS-ST-T

Table 3. The Optimal MCG Channels: QRS Integral, ST-Segment Amplitude, T Wave Amplitude, and ST-T Wave Integral in Separating the MI Groups from the Controls by Use of Departure Index

	All MI	NQMI	QMI
QRS integral			
Departure index	1.53	0.98	2.38
Patients (fTs)	320 ± 350[a]	350 ± 280	430 ± 430[a]
Controls (fTs)	120 ± 130	210 ± 150	120 ± 130
ST-segment amplitude			
Departure index	−1.51	−1.35	−1.83
Patients (fT)	−380 ± 490[b]	−260 ± 480[c]	−550 ± 440[b]
Controls (fT)	290 ± 440	380 ± 470	110 ± 360
T wave amplitude			
Departure index	−2.46	−2.41	−2.54
Patients (fT)	−1600 ± 2200[b]	−880 ± 3500[b]	−1700± 2200[b]
Controls (fT)	1900 ± 1400	3700 ± 1900	1900 ± 1400
ST-T wave integral			
Departure index	−2.47	−2.38	−2.57
Patients (fTs)	−250 ± 300[b]	−230 ± 290[b]	−260 ± 310[b]
Controls (fTs)	200 ± 180	200 ± 180	200 ± 180

[a]$P < 0.05$, [b]$P < 0.001$, [c]$P < 0.005$ comparing patient group to control group; Mann-Whitney U test. Mean ± standard deviation. Abbreviations: MI = myocardial infarction.

angle was not significantly different between the MI group or the NQMI subgroup and the controls. The QRS-ST-T angle was larger in the QMI subgroup than in the controls (QMI subgroup 94 ± 59° and controls 38 ± 46°; $P = 0.011$).

Sums of ECG Parameters Over the 12-Lead ECG

The QRS area was larger in the MI group, in the NQMI group, and in the QMI group than in the controls (MI group 368 ± 731 μVs, controls 98 ± 106 μVs; $P < 0.001$) (Table 4). The ST-segment amplitude, ST-T wave integral, and T wave amplitude did not separate any of the MI groups from the controls.

DISCUSSION

Main Results

The present study showed that several magnetocardiographic repolarization indexes could separate patients with healed MI from the controls. These repolarization abnormalities were more distinct in patients with Q wave-MI than in patients with non-Q wave MI. In the former, they may perform as well as the conventional ECG QRS criteria for detection of healed MI. In patients with non-Q wave MI, a trend similar to patients with Q wave MI was found, but the abnormalities were less distinct. The relation of QRS area to ST-segment, T wave, and ST-T wave integrals improved the detection of healed MI. When comparing the MI patients to the

Table 4. The 12-Lead ECG Variables in Detection of Healed MI

	All MI	P Value	NQMI	P Value	QMI	P Value	Controls
QRS area (μVs)	370 ± 730	<0.001	360 ± 720	<0.001	380 ± 760	<0.001	100 ± 110
ST-segment amplitude (μV)	330 ± 220	n.s.	270 ± 170	n.s.	390 ± 250	n.s.	270 ± 340
ST-T integral (μVs)	270 ± 140	n.s.	270 ± 130	n.s.	280 ± 160	n.s.	250 ± 180
T wave amplitude (μV)	2000 ± 1200	n.s.	2000 ± 1100	n.s.	1900 ± 1300	n.s.	1300 ± 4200

The values are sums of MI parameters of all 12 leads Statistical comparisons are made between the MI, QMI, and NQMI patient groups and the control group.
P values comparing the patient group to the control group; Mann-Whitney U test. Mean ± standard deviation. MI = myocardial infarction; NQMI = non-Q wave myocardial infarction; QMI = Q wave myocardial infarction.

controls, the orientation of the magnetic field differed more in the ST-T wave maps than in the QRS maps.

Comparison of QRS, ST-Segment, and T Wave Parameters

Interestingly, the QRS area summed from the entire recording array was larger in the MI group and in the QMI subgroup than in the controls. The NQMI subgroup showed a similar trend but the difference was not significant. Neither the sums of QRS integral nor ST-segment, T wave, or ST-T wave integrals alone did show discriminative power in differentiating between the MI group and the controls. The ST-segment and ST-T wave integrals did, however, separate the QMI subgroup from the controls. This suggest that repolarization abnormalities are more pronounced in patients with QMI than in patients with NQMI. Earlier MRI studies have shown that the primary determinant of the presence of a Q wave is the total size of underlying territorial MI rather that its transmural extent.[23] Our study thus shows that in QMI the larger myocardial damage induces more secondary repolarization abnormalities, possibly reflecting the more extensive structural alteration, fibrosis, and LV remodeling. These repolarization abnormalities in patients with healed MI should generally not only be interpreted as acute ongoing myocardial ischemia.

In accordance to our study, earlier MI studies have also suggested that in post-MI patients MCG may show information complementary to the ECG especially during the repolarization phase.[24] Van Leeuwen et al. have shown that post-MI patients demonstrate different patterns of spatial QT-time distributions compared to healthy subjects.[25] Kandori et al. have also found abnormalities in the MCG signal during ST-segment in patients with coronary artery disease with or without previous MI.[26] In addition, current density reconstruction maps have shown ST-segment repolarization abnormalities in patients with coronary artery disease but unimpaired LV function.[4]

Optimal Recording Sites

In the optimal recording sites all tested repolarization indexes, in contrast to QRS integral, differentiated between the MI groups and the controls. In the optimal recording sites the repolarization phase thus performed slightly better than the depolarization phase in detection of healed MI. Although the NQMI subgroup demonstrated a trend similar to the QMI subgroup, sums of repolarization indexes in all channels failed to distinguish the NQMI subgroup from the controls. The repolarization abnormalities in the NQMI subgroup are thereby more subtle than the ones in the QMI subgroup, the former only evident in the optimal recording sites, the latter over the whole mapping region. The optimal recording sites for the QRS and ST-T wave indexes did not show extensive variation in between the MI groups, in accord with our earlier studies on exercise-induced transient ischemia.[8]

QRS-ST, QRS-T, and QRS-ST-T Discordance

The QRS-ST, QRS-T, and QRS-ST-T discordance could separate the MI group and the QMI subgroup from the controls, with the AUCs between 70% and 80%. They showed a similar trend also in patients with NQMI. Compared to the ST-segment, T wave, and ST-T wave integrals alone, relating the depolarization and repolarization phases by use of QRS-ST-T discordance improved the performance of the indexes. QRS-ST-T discordance has earlier been applied in detection of LV hypertrophy.[19] In our study, the performance of the QRS-ST-T discordance was dependent on the extent of the known MI damage, with better discriminative power in the QMI subgroup, exhibiting lower LV systolic function and thus more extensive MI damage, than in the NQMI subgroup.

Magnetic Field Map Orientations

The MFM orientation is especially sensitive in reflecting the spatial changes over the MCG mapping area even when the sums of the indexes fail to demonstrate any difference. The present study showed that although the sums of the ST-T wave indexes failed to separate the MI groups from the controls, the ST-T angle distinguished the MI group and the QMI subgroup from the controls. In addition, the QRS-ST-T angle was larger in the QMI subgroup than in the controls, whereas for the NQMI group, in spite of the similar trend, the difference was not significant.

Earlier studies have shown that the MFM orientation changes during exercise-induced myocardial ischemia both in patients with single- and multivessel disease.[7,8] Furthermore, a recent study has

also shown that the QRS-ST-T angle is larger in patients with LV hypertrophy than in healthy controls.[19] To our knowledge, the MFM orientation has not been earlier studied in patients with healed MI. Another MCG study, however, has shown that patients with healed inferior MI have subtle T wave abnormalities in the isomagnetic maps, not detected in ECG.[27]

Future Perspectives

The novel MCG recording systems, operating without expensive magnetic shielding, will permit less expensive MCG measurements without technical limitations even in the clinical environment. Such developments will allow to study also patients with acute MI. Studies comparing MCG with the preexisting methods of ischemia assessment are needed to evaluate its future value in clinical practice.

LIMITATIONS

The percentage of females was larger in the controls than in the MI group. Due to the sexual differences in the repolarization, this disparity may have affected our results. Although none of the study patients had rest angina, in multivessel disease definite exclusion of regional ongoing ischemia was not possible. The sample size was insufficient for analyzing the performance of the various MI indexes in different infarct locations. By use of contrast-enhanced MRI as gold standard, however, we assured that the patient cohort represented infarcts in various locations as well as QMIs and NQMIs. Thus the method allowed inclusion of patients lacking diagnostic findings in standard 12-lead ECG. The Minnesota code classifications therefore merely demonstrated the subclinical nature of the majority of the MIs by conventional ECG analysis. Sensitivity and specificity of the evaluated MI indexes should be assessed in another, larger patient sample, and thus only preliminary conclusions can be made.

CONCLUSIONS

Magnetocardiography can be applied to detect healed MI both in patients with Q wave and in patients with non-Q wave MI. MCG repolarization variables, such as ST-T wave abnormalities, are more pronounced in patients with Q wave MI with more extensive myocardial damage than in patients with non-Q wave MI. Relating the signals of the depolarization and repolarization phases improves the detection of healed MI as compared to either of these signals alone. Finally, repolarization abnormalities in post-MI patients may not only be due to acute myocardial ischemia but also a consequence of previous MI damage.

REFERENCES

1. Bertrand ME, Simoons ML, Fox KAA, et al. Management of acute coronary syndromes in patients presenting without persistent ST-segment elevation. Eur Heart J 2002;23:1809–1840.
2. Siltanen P. Magnetocardiography. In MacFarlane P (ed.): Comprehensive Electrocardiology, Vol. II. New York, Pergamon Press, 1989, pp. 1408–1438.
3. Nenonen J, Montonen J, Mäkijärvi M. Principles of magnetocardiographic mapping. In Shenasa M, Borgreffe M, Breithardt G (eds.): Cardiac Mapping, 2nd Edition. Mount Kisco, NY, Futura Publishing Co., 2002, pp. 119–130.
4. Hailer B, Chaikovsky I, Auth-Eisernitz S, et al. Magnetocardiography in coronary artery disease with a new system in an unshielded setting. Clin Cardiol 2003;26:465–471.
5. Brockmeier K, Schmitz L, Chavez JJB, et al. Magnetocardiography and 32-lead potential mapping: Repolarization in normal subjects during pharmacologically induced stress. J Cardiovasc Electrophysiol 1997;8:615–626.
6. Van Leeuwen P, Hailer B, Lange S, et al. Spatial distribution of repolarization times in patients with coronary artery disease. Pacing Clin Electrophysiol 2003;26:1706–1714.
7. Hänninen H, Takala P, Mäkijärvi M, et al. Detection of exercise induced myocardial ischemia by multichannel magnetocardiography in single vessel coronary artery disease. Ann Noninvasive Electrocardiol 2000;5(2):147–157.
8. Hänninen H, Takala P, Korhonen P, et al. Features of ST segment and T-wave in exercise-induced myocardial ischemia evaluated with multichannel magnetocardiography. Ann Med 2002;34:120–129.
9. Kanzaki H, Nakatani S, Kandori A, et al. A new screening method to diagnose coronary artery disease using multichannel magnetocardiogram and simple exercise. Basic Res Cardiol 2003;98:124–132.
10. Gerber BL, Garot J, Blumeke DA, et al. Accuracy of contrast-enhanced magnetic resonance imaging in predicting improvement of regional myocardial function in patients with acute myocardial infarction. Circulation 2002;106:1083–1089.
11. Prineas RJ, Crow RS, Blackburn H. The Minnesota Code Manual of Electrocardiographic Findings, Standards and Procedures for Measurement and Classification. Bristol, Wright, 1982.
12. Cerquiera MC, Weissman NJ, Dilsizian V, et al. Standardized myocardial segmentation and nomenclature for tomographic imaging of the heart. Circulation 2002;105:539–542.
13. Brunken R, Schwaiger M, Grover-McKay M, et al. Positron emission tomography detects tissue metabolic activity in myocardial segments with persistent thallium perfusion defects. J Am Coll Cardiol 1987;10:557–567.
14. Knuuti MJ, Nuutila P, Ruotsalainen U, et al. Euglycemic hyperinsulinemic clamp and oral glucose load in stimulating myocardial glucose utilization during positron emission tomography. J Nucl Med 1992;33:1255–1262.
15. Nenonen J. Multimodal cardiac source imaging in the BioMag laboratory. Biomed Tech (Berl) 1997;42:29–43.

16. Burghoff M, Nenonen J, Trahms L, et al. Conversion of the magnetocardiographic recordings between two different multichannel SQUID devices. IEEE Trans Biomed Eng 2000;42:72–78.
17. Simson MB. Use of signals in the terminal QRS complex to identify patients with ventricular tachycardia after myocardial infarction. Circulation 1981;64:235–242.
18. Oikarinen L, Paavola M, Montonen J, et al. Magnetocardiographic QT interval dispersion in postmyocardial infarction patients with sustained ventricular tachycardia: Validation of automated QT measurements. Pacing Clin Electrophysiol 1998;21:1934–1942.
19. Karvonen M, Oikarinen L, Takala P, et al. Magnetocardiographic indices of left ventricular hypertrophy. J Hypertens 2002;20:2285–2292.
20. Thiry PS, Rosenberg RM, Abbott JA. A mechanism for the electrocardiogram response to left ventricular hypertrophy and acute ischemia. Circ Res 1975;36:92–104.
21. Flowers NC, Horan LG, Johnson JC. Anterior infarctional changes occurring during mid and late ventricular activation detectable by surface mapping techniques. Circulation 1976;54:906–913.
22. Flowers NC, Horan LG. Body surface potential mapping. In Zipes DP, Jalife J (eds.): Cardiac Electrophysiology: From Cell to Bedside, 2nd Edition, Philadelphia, WB Saunders Company, 1995, pp. 1049–1067.
23. Moon JCC, De Arenaza DP, Elkington AG, et al. The pathological basis of Q-wave and non-Q-wave myocardial infarction. A cardiovascular magnetic resonance study. J Am Coll Cardiol 2004;44:554–560.
24. Lant J, Stroink G, ten Voorde B, et al. Complementary nature of electrocardiographic and magnetocardiographic data in patients with ischemic heart disease. J Electrocardiol 1990;23:315–322.
25. Van Leeuwen P, Hailer B, Wehr M. Spatial distribution of QT intervals: An alternative approach to QT dispersion. Pacing Clin Electrophysiol 1996;19(Pt. II):1894–1899.
26. Kandori A, Kanzaki H, Miyatake K, et al. A method for detecting myocardial abnormality by using a total current-vector calculated from ST-segment deviation of a magnetocardiogram signal. Med Biol Eng Comput 2001;39:21–28.
27. Nomura M, Nakaya Y, Fujino K, et al. Magnetocardiographic studies of ventricular repolarization in old inferior myocardial infarction. Eur Heart J 1989;10:8–15.